Cascade-exciton model analysis of mass dependence of pion-induced fission

Muhammad Ikram Shahzad[1;1)] Zafar Yasin[1] Warda Iram[2] Shahida Jabeen[3]

[1] Physics Division, PINSTECH, P.O. Nilore, Islamabad, Pakistan
[2] Physics Department, Islamia University, Bahawalpur, Pakistan
[3] Physics Department, AJ&K University, Muzaffarbad, Pakistan

Abstract: The cascade-exciton model has been used to observe the dependence of pion induced fission cross sections on the mass of the target. The analysis has been performed at energies 80 MeV, 100 MeV and 150 MeV for both the positive and negative pions. It has been shown that a single value of the ratio $a_{\rm f}/a_{\rm n}$ can satisfactorily reproduce the experimental findings when compared with the available experimental data in the literature. The general trend of the fission cross sections with mass (fissility parameter) is seen to be low and slowly changing for the lighter nuclei, and it will steeply rise for the heavy nuclei.

Key words: cascade-exciton model, pion-induced fission, cross sections

PACS: 24.75.+i, 25.85.-w, 25.80.-e **DOI:** 10.1088/1674-1137/38/7/076101

1 Introduction

Since the first observation of nuclear fission, it has played a pivot role in exploring the fundamentals of nuclear physics [1–4]. It has gained prominent importance in the conventional and current nuclear applications [5], such as cascades in heavy nuclear spallation targets, which are partly propagated by pions. Pion induced nuclear reactions, particularly fission reactions, have not been studied as extensively as other probes. For many applications in nuclear science & technology, fission reactions induced by pions are as imperative as other fission invoking channels, such as nucleon and photon induced nuclear reactions [6]. As field particles of nuclear force, pions are important ingredients of nuclear reactions at intermediate energies. Their couplings to major nuclear de-excitation modes are major causes of the final reaction channel [6]. Pion induced nuclear reactions are of novel nature because the rest mass energy of pion (~140 MeV) is fully absorbed by the colliding nucleons and the energy transferred spreads over the rest of the fast moving interacting nucleonic system [7]. Moreover, pions, as the field particles of nuclear force, mediate not only the forces among the nucleons but also act as intermediate step for nuclear reactions invoked by other intermediate energy probes, such as antiprotons, heavy ions, photons, etc. [8].

The nuclear fission cross sections strongly depend on the incident energy of the projectile and masses of projectile & target. We have performed a comparison of pion and proton induced fission in our previous studies [6, 9] and have concluded that, at the same excitation energies, pion induced fission is similar to proton induced fission. It has also been observed experimentally that, in case of light target nuclei (e.g. tin) the fission cross sections increase with the energy of the pion, up to the available energy range [3]. For elements such as gold and bismuth, the fission cross sections show a saturation with the beam energy [1, 3, 6]. For heavy nuclei, such as uranium, a decrease of fission cross section has been observed at higher energies [2].

The analytical results of mass dependence of pion induced fission cross-section are reported in this paper. The theoretical results from the study of mass dependence of pion induced fission have not been reported earlier, even using the Cascade-Excition Model (CEM). There is a lack of information relating the role of pion sign in the change of the fissility parameter from Z^2/A to $(Z\pm1)^2/A$. The limited availability of experimental results related to the intensity effects of pion beams is also an important shortcoming in the studies of pion induced fission as compared to fission induced by other probes. The production of pions in p-p or Pb-Pb collisions at LHC, CERN has increased the importance of pion and nucleon induced nuclear reaction data. The pions produced at LHC energies induce different types of reactions in the experimental set-ups (e.g. ALICE, CMS, ATLAS, etc.) by interacting with the materials of the detectors

Received 17 June 2013

1) E-mail: mshahzad@cern.ch; mishahzad58@yahoo.com

and their sub-detectors. Therefore, a large amount of data is required for these invoked pion induced reaction channels to simulate the physics and geometry of the detectors.

In the literature the experimental data of pion induced reaction cross sections are not available as compared to the data that is available for nucleons and photons Therefore, different theoretical models and computer codes are essential tools for the study of basic and applied nuclear physics, as well as for high energy physics. This paper presents the results of the calculations that we performed using the cascade-exciton model. In the present work, for one energy of incident pions, the trend of computed cross sections for two values of the ratio of level density parameters, $a_{\rm f}/a_{\rm n}$ has been studied. It is observed that a single value of $a_{\rm f}/a_{\rm n}$ can describe well the mass dependence of pion induced fission cross sections when compared with the experimental data.

2 Simulation of fission cross sections

The cascade-exciton model based computer code CEM95 [10] has been used because of its good predictive power and extensive employment to calculate the nuclear fission induced by negative and positive pions [1–4, 11–13]. Both the fission cross-sections and probabilities have been computed on the basis of cascade-exciton model of nuclear reactions [14] using this computer code.

Monte Carlo calculations by means of the statistical functions have been performed to compute the fission cross sections. The fission probabilities are estimated as [10],

$$\sigma_{\rm f}=\frac{\sigma_{\rm in}}{N_{\rm in}}\sum_{i=1}^{N_{\rm in}}(W_{\rm f})_i,$$

where $W_{\rm f}$ is the probability for the nucleus to fission at any of the chain stages, $N_{\rm in}$ is the total number of the cascades followed, and $\sigma_{\rm in}$ is the total inelastic cross section.

The partial widths $\Gamma_{\rm j}$ for the emission of a particle j (j=n, p, d, t, ^{3}He, ^{4}He) and $\Gamma_{\rm f}$ for fission are given by the expressions;

$$\Gamma_{\rm j}=\frac{(2s_{\rm j}+1)m_{\rm j}}{\pi^2\rho_{\rm c}(U_{\rm c})}\int_{V_{\rm j}}^{U_{\rm j}-B_{\rm j}}\sigma_{\rm inv}^{\rm j}(E)\rho_{\rm j}(U_{\rm j}-B_{\rm j}-E)E{\rm d}E$$

and

$$\Gamma_{\rm f}=\frac{1}{2\pi\rho_{\rm c}(U_{\rm c})}\int_0^{U_{\rm f}-B_{\rm f}}\rho_{\rm f}(U_{\rm f}-B_{\rm f}-E)E{\rm d}E,$$

where

$\rho_{\rm c}$=level density of the compound nucleus;

$\rho_{\rm j}$=level density of the compound nucleus produced after the emission of particle j;

$\rho_{\rm f}$=level density of the fissioning nucleus at the fission saddle point;

$m_{\rm j},s_{\rm j},B_{\rm j}$=mass, spin, and binding energy of particle j, respectively; and,

$\sigma_{\rm inv}^{\rm j}(E)$= inverse cross section for absorption of particle j with kinetic energy E by the residual nucleus. The thermal energies $U_{\rm k}$ are defined by

$$U_{\rm c}=E^*-E_{\rm R}^{\rm c}-\Delta_{\rm c},$$
$$U_{\rm j}=E^*-E_{\rm R}^{\rm j}-\Delta_{\rm j},$$
$$U_{\rm f}=E^*-E_{\rm R}^{\rm sp}-\Delta_{\rm f},$$

where E^* is the total excitation of the compound nucleus, and $E_{\rm R}^{\rm c}$ and $E_{\rm R}^{\rm j}$ are the rotational energies of the compound and residual nuclei at their ground states.

The cascade stage of the interaction is described by the Dubna version of the Intranuclear Cascade Model (ICM) [15]. Besides the elementary process, the Dubna ICM also takes into account the pion absorption on the nuclear pairs NN (for a nucleus N);

$\pi{\rm NN}\longrightarrow{\rm NN}$.

The momenta of two nucleons participating in the absorption are chosen randomly from the Fermi distribution. The pion energy is distributed equally between these nucleons in the center-of-mass system of the pion and nucleons participating in the absorption. The direction of motion of the resultant nucleons is considered to be isotropic.

For the CEM and for the other models, the most important values are those of the level density parameters, $a_{\rm f}$ and $a_{\rm n}$, for the saddle point of fission and equilibrium deformation of the nucleus.

Previously CEM95 code has been used in a new manner for the study of pion and nucleon induced fission cross-sections and it was observed that the energy dependence of fission cross sections is very sensitive to the ratio $a_{\rm f}/a_{\rm n}$ [1, 13]. The best value for this ratio is still one of the most important issues in the research of nuclear physics [16–18].

In our previous studies, the value of $a_{\rm f}/a_{\rm n}$ has been selected by keeping in mind the values evaluated by Iljinov [19], whose calculations were for zero energy pions ($a_{\rm f}/a_{\rm n}$=1.2) and energetic protons at incident energies of 150 MeV ($a_{\rm f}/a_{\rm n}$=1.17), 660 MeV ($a_{\rm f}/a_{\rm n}$ =1.06), and 1000 MeV ($a_{\rm f}/a_{\rm n}$=1.04).

In the present study, we have observed that the trend of mass dependence of fission cross sections as compared to the experimental data is not very sensitive to the value of $a_{\rm f}/a_{\rm n}$. It has been analyzed that a single value of $a_{\rm f}/a_{\rm n}$ (i.e. 1.2) can describe well the mass dependence of pion induced fission cross sections at energies of 80 MeV, 100 MeV, and 150 MeV. The comparison of two different values of $a_{\rm f}/a_{\rm n}$ (i.e. 1.2 and 1.29) has been also shown for 100 MeV pion energy. The reason for the selection of beam energies at 80 MeV, 100 MeV, and 150 MeV is that these values lie down where the delta resonance is expected to be dominant. Moreover, the experimental data are also available at these energies, which can be used for comparison.

3 Results and discussion

The mass dependence at 80 MeV of π^+ and π^- induced fission cross sections computed using CEM95 is shown in Figs. 1 and 2, respectively. The cross sections are plotted against the fissility parameter, $(Z+1)^2/A$ for π^+ and $(Z-1)^2/A$ for π^-. The solid lines are the fission cross sections by $\pi^{\pm}$, computed using CEM95, and the squares are the experimental data points taken from literature.

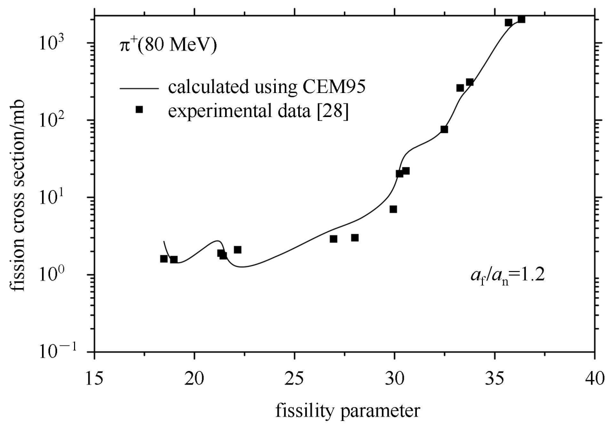

Fig. 1. Fissility parameter, $(Z+1)^2/A$, dependence of positive pion induced fission cross sections for 80 MeV.

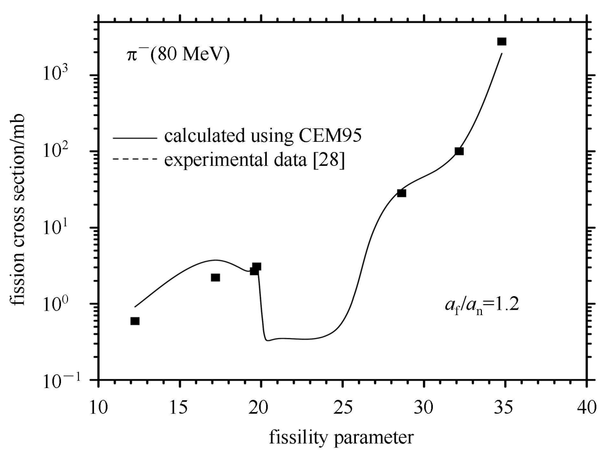

Fig. 2. Fissility parameter, $(Z-1)^2/A$, dependence of negative pion induced fission cross sections for 80 MeV.

The calculated cross sections show reasonable agreement with the experimental data. The cross sections show a slowly changing trend up to the fissility parameter 28–29 for lighter nuclei, but then exhibit a steep rise with the fissility parameter above 29. A dip in the computed cross sections is noted in the fissility parameter range 25–29. The same kind of dip has been observed in the other analyses, as can be seen in Figs. 18 and 34 of Ref. [20]. In this work we have observed that the values of computed cross sections for fission are the most appropriate for all the nuclei using a single value of a_f/a_n (i.e 1.2). The other important parameters that we have used are: the third Iljinov et al. systematics for the level density parameters [21]; the fission barriers of Krappe, Nix, and Sierk [22]; and, Truran, Cameron and Hilf's shell corrections [23].

The mass dependence at 100 MeV of π^+ and π^- induced fission cross sections is shown in Fig. 3 and Ref. [4] respectively. The cross sections are plotted against the fissility parameter, $(Z+1)^2/A$ for π^+ and $(Z-1)^2/A$ for π^-. The solid and dashed lines are the calculations made by the CEM95 and the squares are the experimental data points.

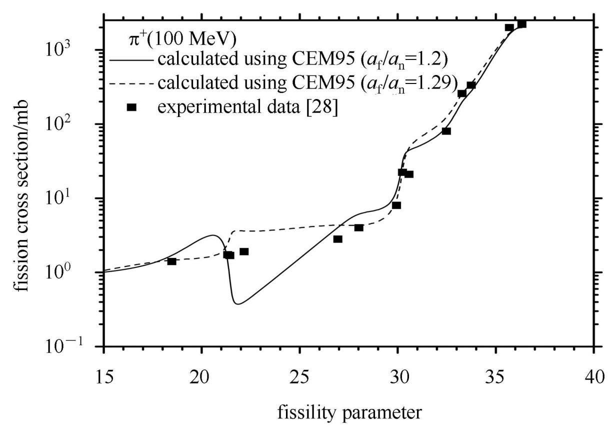

Fig. 3. Fissility parameter, $(Z+1)^2/A$, dependence of positive pion induced fission cross sections for 100 MeV.

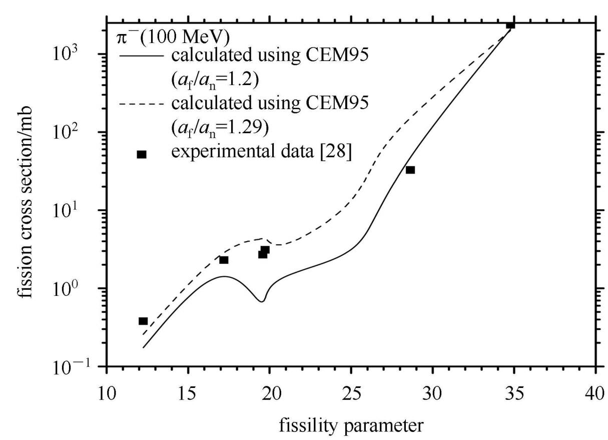

Fig. 4. Fissility parameter, $(Z-1)^2/A$, dependence of negative pion induced fission cross sections for 100 MeV.

The calculated cross sections are in reasonable agreement with the experimental data. At this energy, the cross sections show a slowly changing trend up to the fissility parameter 29.44 for lighter nuclei, but then indicate a steep rise with the fissility parameter above 29.44. A notable dip in the computed cross sections is noted in the fissility parameter range 25–30 for π^+ and very small dip for π^- in the same range. For comparison, two values of a_f/a_n (i.e 1.2 & 1.29, respectively) have been shown in Figs. 3 and 4. Here, the calculations are also found to be most appropriate for value of $a_f/a_n = 1.2$ for all the nuclei. The other important CEM95 parameters used are: the third Iljinov et al. [21] systematics for the level density parameters; the fission barriers of Krappe, Nix, and Sierk; and, Truran [22], Cameron and Hilf's shell corrections [23].

At 150 MeV pion energy, the mass dependence of π^+ and π^- induced fission cross sections have been shown in Figs. 5 and 6, respectively. The cross sections are plotted against the fissility parameter, $(Z+1)^2/A$ for π^+ and $(Z-1)^2/A$ for π^-.

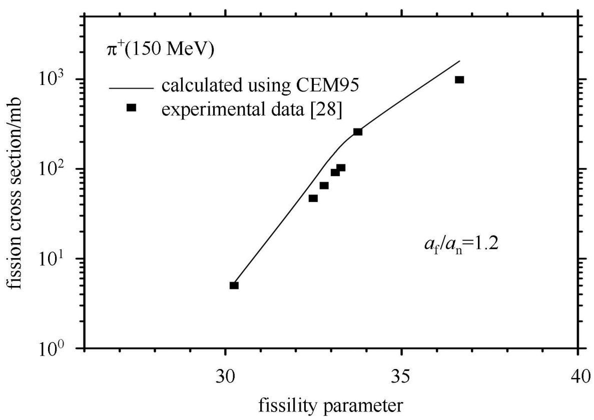

Fig. 5. Fissility parameter, $(Z+1)^2/A$, dependence of positive pion induced fission cross sections for 150 MeV.

The computed predictions show reasonable agreement with the experimental data. The curves indicate the smooth upward trends of fission cross sections with the target mass. The rapid increase of cross sections with mass is directly correlated with the strong decrease of fission barriers with mass, as also indicated in Ref. [24, 25].

The excitation energy dependence of fission barriers is taken into account, for ^{181}Ta, ^{197}Au, ^{205}Tl and ^{231}Pa proposed by Sauer, Chandra, and Mosel [26], and for other nuclei proposed by Barashenkov, Gereghi, Iljinov and Toneev [27]. For all the nuclei, except ^{231}Pa, the calculations are performed with a single humped fission barrier and for ^{231}Pa with double humped fission barrier. For all the nuclei, the other important CEM95 parameters that we have used are: the third Iljinov et al. systematics for the level density parameters [21]; the fission barriers of Krappe, Nix, and Sierk [22]; and, Turan, Cameron and Hilf's shell corrections [23].

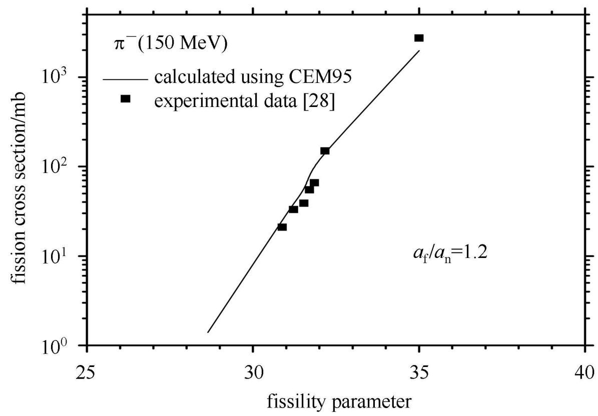

Fig. 6. Fissility parameter, $(Z-1)^2/A$, dependence of negative pion induced fission cross sections for 150 MeV.

4 Conclusions

The mass dependence of pion induced fission cross sections in the intermediate energy range and across the delta resonance has been studied using the cascaded-exciton model computer code CEM95. The computed cross sections for fission are in reasonable agreement with the experimental data from the literature. For lighter nuclei, the cross sections show a low and slowly changing trend following a sharp increasing trend with the mass of the target. The main conclusion in our present study is that a single value of a_f/a_n can well describe the mass dependence of pion induced fission and this methodology can be used to compute cross sections for nuclei for which no experimental data is available.

The authors are thankful to Prof. R. J. Peterson for useful technical discussions and advice to improve this manuscript. We also acknowledge the computational help and assistance provided by Mr. Bashir Ahmad Shad.

References

1 Yasin Z, Shahzad M I, Qureshi I E, Sher G, Peterson R J. Nucl. Phys. A, 2006, **765**: 390
2 Yasin Z, Shahzad M I. Nucl. Phys. A, 2006, **773**: 221
3 Yasin Z, Shahzad M I, Peterson R J, Sher G, Javed M T, Khan H A. Nucl. Phys. A, 2007, **781**: 296
4 Yasin Z, Shahzad M I, Khan H A, Peterson R J, Asghar M. Radiation Measurements. 2008, **43**: S174
5 Yasin Z, Shahzad M I. Ann. Nucl. Energy, 2010, **37**: 87
6 Yasin Z, Shahzad M I, Khan H A, Peterson R J, Schroder B. Radiation Measurements, 2009, **44**: 846
7 Tanabe K. Prog. Theor. Phys., 1997, **61**: 354
8 Arruda-Neto J D T, Saito T, Sugawara M, Tamae T, Miyase H, Abe K, Konno O, Oikawa M, Simionatto S, Yoneama M L, Dias J F, Deppman A, Bhandari B S, Likhachev V P, Lima A CS. Phys. Rev. C, 1996, **54**: 3294
9 Hicks K H, Jeppesen R G, Kraushaar J J, Kunz P D, Peterson R J, Raymond R S, Ristinen R A, Ullmann J L, Becchetti F D, Bradbury J N, Paciotti M. Phys. Rev. C, 1985, **31**: 1323
10 Mashnik S G. Computer Code CEM95. OECD Nuclear Energy Agency Data Bank, Paris, France, 1995
11 Mashnik S G. Acta Phys. Slovaca, 1993, **43**: 86
12 Mashnik S G. Acta Phys. Slovaca, 1993, **43**: 243
13 Yasin Z. Chin. Phys. Lett., 2009, **26**(082595): 1–4
14 Gudima K K, Mashnik S G, Toneev V D. Nucl. Phys. A, 1983, **401**: 329
15 Vandenbosch R, Huizenga J R. Academic Press, 1973
16 Aydin A, Yalim H A, Tel E, Şarer B, Ünal R, Sarpün İ H, Kaplan A, Dağ M. Ann. Nucl. Energy, 2009, **36**: 1307
17 Iljinov A S, Cherepanov E A, Chigrinov S E. Z. Physik A, 1978, **287**: 37
18 Tavares O A P, Medeiros E L. J. Phys. G. Nucl. Part. Phys., 2004, **30**: 395
19 Iljinov A S, Cherepanov E A, Chigrinov S E. Sov. J. Nucl. Phy., 1980, **32**: 166
20 Peterson R J. Journal of Nuclear and Radiochemical Sciences, 2010, **11**: R1
21 Iljinov A S, Mebel M V, Bianchi N, de Sanctis E, Guardalo C, Lucherini V, Muccifora V, Polli E, Reolon A R, Rossi P. Nucl. Phys. A, 1992, **543**: 517
22 Krappe H J, Nix J R, Sierk A J. Phys. Rev. C, 1997, **20**: 992
23 Truran J W, Cameron A G W, Hilf E. Proc. Int. Conf. on the Properties of Nuclei Far from the Region of Beta-Stability. Leysin, Switzerland, 1970, **1**: 275
24 de Barros S, da Silva A G, Suita J C, Peterson R J. Z. Phys. A, 1997, **359**: 35
25 Gadioli E, Ebra E G, Moroni A. Z. Phys. A, 1978, **288**: 39
26 Sauer G, Chandra H, Mosel U. Nucl. Phys. A, 1976, **264**: 221
27 Barashenkov V S, Gereghi F G, Iljinov A S, Toneev V D. Nucl. Phys. A, 1974, **222**: 204
28 Peterson R J, de Barros S, de Souza I O, Gasper M B, Khan H A, Manzoor S. Z. Phys. A, 1995, **352**: 181